Article

Magnetizable Membranes Based on Cotton Microfibers, Honey, Carbonyl Iron, and Silver Nanoparticles: Effects of Static Magnetic Fields and Medium-Frequency Electric Fields on Electrical Properties

Ioan Bica [1,2] **, Eugen Mircea Anitas** [3,4,]* **and Paula Sfirloaga** [5]

[1] Faculty of Physics, West University of Timisoara, V. Parvan Avenue 4, 300223 Timisoara, Romania
[2] Department of Physics, Craiova University, A. I. Cuza Street 13, 200585 Craiova, Romania
[3] Bogoliubov Laboratory of Theoretical Physics, Joint Institute for Nuclear Research, 141980 Dubna, Russian
[4] Department of Nuclear Physics, Horia Hulubei, National Institute of Physics and Nuclear Engineering, 077125 Bucharest-Magurele, Romania
[5] Department of Condensed Matter, National Institute for Research and Development in Electrochemistry and Condensed Matter, 300224 Timisoara, Romania
[*] Correspondence: anitas@theor.jinr.ru

Abstract: In this work, we present the manufacturing process of magnetizable membranes based on cotton microfibers, honey, carbonyl iron, and three different concentrations of silver microparticles. Each membrane is used as a dielectric material for the fabrication of electrical devices. By using the plane capacitor method, the electrical capacitance and dielectric loss tangent are measured in a medium-frequency alternating field superimposed on a static magnetic field. From the obtained data, the time constants of the devices, the components of complex dielectric permittivity, and the electrical conductivity of the membranes as a function of the electric field frequency and magnetic flux density can be extracted. The results show that the obtained membranes can be useful for the fabrication of low-cost and environmentally friendly magneto-active membranes that are required for various technical and biomedical applications.

Keywords: magnetizable membrane; cotton microfibers; honey; carbonyl iron; silver; electrical properties

1. Introduction

Composite membranes (CMs) are complex structures that consist of two or more materials confined to a spatial arrangement in which one dimension is much smaller than the others [1,2]. The constituent materials have very different chemical and physical properties and one of them, known as the reinforcement, is used as a matrix that fixes the relative positions of the others. The physical and mechanical properties of the membrane are generally improved compared to the individual components since the properties of the matrix are also improved due to the presence of the reinforcement [3,4].

The most common membranes use polymers as the matrix (e.g., epoxy, polyester, polypropylene) and fibers as the reinforcement (e.g., glass, carbon, aramid). This gives rise to high-performance membranes, which are light and yet mechanically very strong, that can be used for various applications in industry, medicine, and people's daily lives [5]. As such, they are often used to remove hazardous contaminants from wastewater [6], in battery and fuel cells [7], in the manufacturing of valuable biomaterials from food waste [8], or for water, gas, and ion separation [9].

However, the ever-increasing needs of modern society require new types of membranes whose properties can be tuned remotely [10]. To this aim, promising candidates

are magnetizable CMs, i.e., membranes in which the reinforcement is a magnetic material [11]. They have been successfully used for electromagnetic wave absorption [12], the enhanced performance of selectivity and separation indexes [13], and information storage and anti-counterfeit measures [14].

In recent years, attention has been focused on biocompatible and environmentally friendly magnetizable CMs in which the matrix is made of natural fibers [15], where the commonly used materials are silk [16], keratin [17], cellulose [18], and cotton [19]. Silk is a fibrous protein in which the hydrophobic side chains consist mostly of glycine, alanine, and serine that form β-sheets responsible for its high tensile strength. Thus, they are suitable for use as tissue scaffolds [20]. Keratin is a cysteine-rich biopolymer in which two α-helices form a superhelix structure by winding around each other. They also have good mechanical properties, and due to their natural abundance, they are found in many applications [21]. Cellulose is a structural polysaccharide in which the fibers are formed by joining glucose through intramolecular hydrogen bonding. This leads to the formation of rigid fibers which, when treated with sodium hydroxide, become very stable thermodynamically [20,21].

Cotton fibers are made up of cellulose with 1,4-glucopyranose structural units that further enhance their performance and make them compatible with other surfaces [22]. They have a fibrilar structure consisting of a primary wall surrounding a secondary one that, in turn, embodies the lumen [23]. The main properties, processing, and use of cotton fibers arise mostly due to the surface layer (cuticle) of the primary wall. Thus, magnetizable CMs based on cotton fibers are useful for applications that require the long-term stability of the structural properties, such as in the fabrication of various electrical devices [24–28].

In this work, we manufacture new low-cost, biodegradable, and efficient magnetizable CMs based on raw natural components: cotton microfibers, honey, carbonyl iron (CI), and silver microparticles. Cotton microfibers are found in most common textiles and they are often modified for durable antibacterial activity, biosecurity, and a comfortable feel [29]. Here, the cotton microfibers used are from sterile gauze bandages made from pure cotton. Their role is to absorb the viscous solution made from honey, CI, and silver nanoparticles. Honey is a natural product that is well known for its therapeutic properties due to its anti-inflammatory and antiseptic properties and is widely used as food support in the form of bee products [30]. CI is a biodegradable industrial product that has been commercialized in the form of powder and is often used for the manufacturing of new materials, such as magnetorheological suspensions [31] and elastomers [32], as well as in biomedical applications [33], e.g., for the prevention/treatment of iron-deficiency anemia [34]. This silver powder in the form of nano- and microparticles is also biodegradable and is useful for making electromagnetic radiation-absorbent layers. In the magnetizable CMs obtained here, the silver microparticles have a role in inducing pre-established conductibility and creating an environment with anti-inflammatory and antimicrobial properties. Thus, compared to other magnetizable CMs reported in the literature [11–15,24–28], here, the addition of silver makes the obtained membrane superior for various biomedical applications such as dermatological or dental treatments [35].

By using the obtained membranes as dielectric materials inside an electrical device in the form of a plane capacitor, we investigate their electrical properties using a new experimental setup that is described here. As such, the electrical capacitance and the tangent of the dielectric loss angle in a medium-frequency electric field superimposed on a static magnetic field are measured. The role of the magnetic field is twofold. First, it induces magnetic interactions inside the composite such that the material properties are changed almost instantaneously from its application. Second, for well-chosen values of the magnetic flux density, it plays a preventive role. The obtained information is further used to study the time constant of the device, components of the dielectric permittivity, and electrical conductivity of the membranes. The results show that the electrical properties can be preset in advance by choosing the right number of components and they are noticeably influenced by both the electric and magnetic fields, thus making them suitable

for electromagnetic shielding and the electrically and/or magnetically induced release of the bioactive compounds from honey.

2. Materials and Methods

The materials used for the fabrication of magnetizable CMs were as follows:

- Cotton microfibers made from sterile compression from Labormed Pharma S.A. in the form of gauze bandages (GB) manufactured by Shaoxing Gangfeng Hospital Products Co Ltd (China)(company, city, state, country), with threads of 100% pure cotton (Figure 1a). The mass density of the cotton microfibers was $\rho_{CmF} = 0.735$ g/cm^3 at 22°, with a relative air humidity of 60 %.
- Lime honey with good antimicrobial and anti-inflammatory properties, which was obtained from bee harvests from lands with linden forests. The mass density was $\rho_H = 1.496$ g/cm^3 at 22°.
- CI microparticles from Sigma-Aldrich Chemie GmbH (Taufkirchen, Germany), product code C-3518(city, state, country), with a minimum purity of 99.7 %. The particles had a spherical shape, with an average diameter of $d_{CI} \simeq 5$ μm. The bulk density was $\rho_{CI} = 3.512$ g/cm^3 at 22°.
- Silver microparticles from Sigma-Aldrich, Saint Louis, (Missouri, USA), product code 327085 (city, state, country)with a purity of at least 99.9 %. The particles also had a spherical shape and an average diameter of $d_S \simeq 3$ μm at 22°. The bulk density was $\rho_S = 1.336$ g/cm^3 at 22°.

(a)   (b)
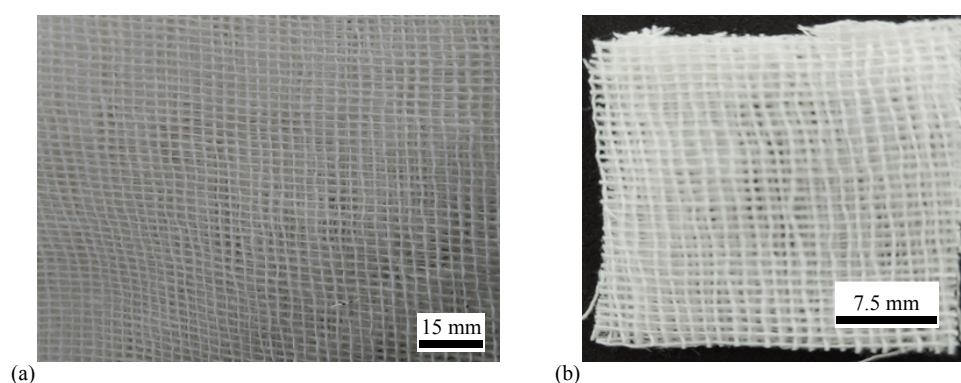
Figure 1. (**a**) Sterile compression of cotton microfibers. (**b**) Sterile compression pack of cotton microfibers.

The main steps for the fabrication of magnetizable CMs were as follows:

1. The sterile compression shown in Figure 1a shows cut pieces with dimensions of 30 mm × 25 mm × 0.80 mm and seven packages were formed. An image of a single package is shown in Figure 1b. The mass of each package was $m_{GB} = 0.200$ g. Thus, the volume of the microfibers within each package was $V_{CmF} = m_{CmF}/\rho_{CmF} = 0.28$ cm^3.
2. Seven magnetic liquid suspensions were prepared in Berzelius glasses at various quantities of honey, CI, and silver microparticles, with the volumes and mass fractions listed in Table 1.
3. The sterile compressions were soaked with the suspensions and the composite membranes M_i, with $i = 1, \ldots, 7$ obtained (see Table 1 and Figure 2). As such, each membrane, except for M_1, contained honey; membranes M_3, M_6, and M_7 contained silver microparticles, and membranes M_4, M_5, M_6, and M_7 contained CI microparticles. The dimensions of each membrane are listed in Table 2.

Table 1. Composition of membranes M_i, with $i = 1, \ldots, 7$. V_{CmF}, V_H, V_S, and V_{CI} are the volumes (in cm^3) of the cotton microfibers, honey, silver microparticles, and CI microparticles, respectively, and Φ_{CmF}, Φ_H, Φ_S, and Φ_{CI} are their respective volume fractions (in *vol*.%).

Membrane	V_{CmF}	V_H	V_S	V_{CI}	Φ_{CmF}	Φ_H	Φ_S	Φ_{CI}
M_1	0.28	0.00	0.00	0.00	0.00	0.00	0.00	0.00
M_2	0.28	0.34	0.00	0.00	45.0	55.0	0.00	0.00
M_3	0.28	0.34	0.10	0.00	39.0	47.0	14.0	0.00
M_4	0.28	0.34	0.00	0.10	39.0	47.0	0.00	14.0
M_5	0.28	0.34	0.00	0.20	34.0	41.0	0.00	24.0
M_6	0.28	0.34	0.10	0.10	34.0	42.0	12.0	12.0
M_7	0.28	0.34	0.10	0.20	30.0	37.0	11.0	12.0

Table 2. Dimensions of the membranes. V, S, and D are the volume, surface, and thickness, respectively.

Membrane	V (cm^3)	S (cm^2)	d (cm)
M_1	0.28	7.50	0.037
M_2	0.62	7.50	0.082
M_3	0.72	7.50	0.096
M_4	0.72	7.50	0.096
M_5	0.82	7.50	0.109
M_6	0.82	7.50	0.109
M_7	0.92	7.50	0.122

(a)   (b)   (c)
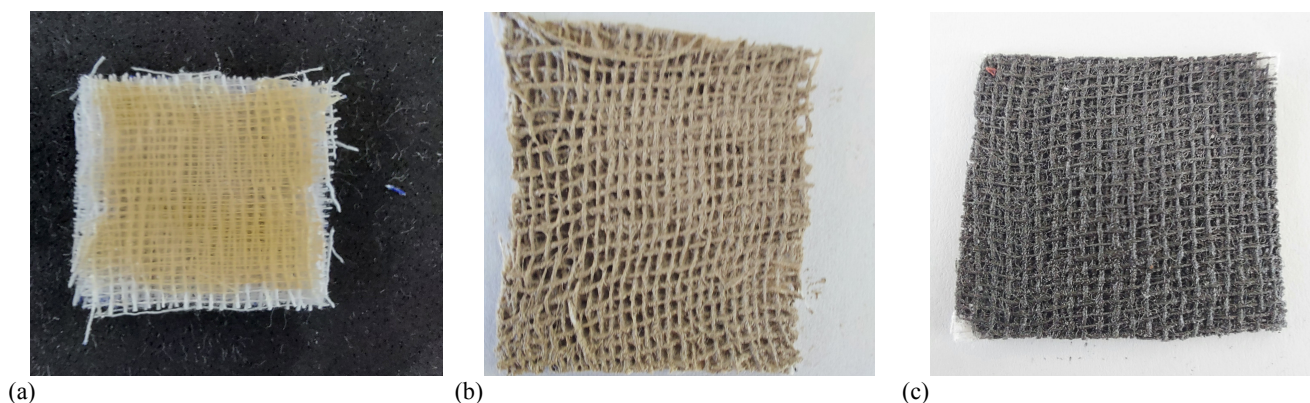
Figure 2. Images of membranes: (**a**) M_2, i.e., only with honey, (**b**) M_3, i.e., with honey and silver microparticles, and (**c**) M_4 , i.e., with honey and CI microparticles. The dimensions of all membranes are the same at 30 mm $\times$ 25 mm (see text for details). Membrane M_1 is shown in Figure 1b. The other membranes (M_5, M_6, and M_7) are similar to M_4.

3. Optical Microscopy

Optical microscopy was performed on the various membranes by using a B-290 series microscope from Optika SRL (Ponteranica, Italy), to illustrate the structure of the cotton microfibers–CI/silver microparticle complex. First, the images of the pure cotton microfibers (M_1) are presented in Figure 3a and it can be seen that the average thickness is about 20 µm. Second, the images of the cotton microfibers with honey and silver microparticles (M_3) show that the latter were attached to the cotton microfibers (Figure 3b). Finally, the images of the cotton microfibers with honey, silver, and CI microparticles (M_4) show that the latter were also attached to the cotton microfibers (Figure 3c).

Figure 3. Optical microscopy images of magnetizable CMs. (**a**) Cotton microfibers (M_1). (**b**) Cotton microfibers with honey (light blue) and silver microparticles (gray spots on cotton microfibers) (M_3). (**c**) Cotton microfibers with honey (light blue), silver microparticles (gray spots on cotton microfibers), and CI (dark spots) (M_4). See the main text and Table 2 for details.

4. Microstructural Characterization and Elemental Analysis

In order to highlight the surface morphologies and elemental compositions of the obtained samples, an electronic scanning microscope Inspect S (SEM) from FEI Europe B.V., Eindhoven, The Netherlands, equipped with an X-ray energy-dispersive spectrometer (EDX) was used. All studied samples were analyzed in low vacuum mode using the LFD detector , with a spot value of 3.5, pressure of 30 Pa, and a high voltage of 30 kV.

The results are presented in Figures 3 and 4 and show that the CI and silver microparticles adhered to the cotton microfibers. They were linked to the cotton microfibers through the honey and absorbed by capillarity in the microfibers' cavities and the spaces between the microfibers of the cotton thread. Elemental analysis showed the presence of a high content of Fe (Figure 4c). Together with Fe, the EDX spectra showed the presence of other elements, such as C, O, and Ag, as expected.
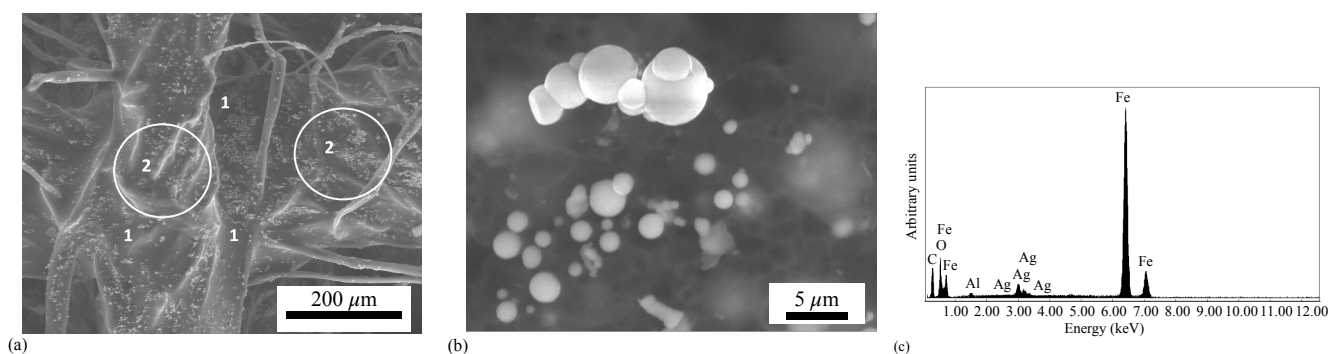

Figure 4. SEM and EDX data of the membrane with honey, CI, and silver nanoparticles (M_6). (**a**) 1—Cotton microfibers, 2—Honey with CI and silver microparticles. (**b**) Largest spheres—CI microparticles; smaller spheres—silver microparticles. (**c**) Elemental analysis.

5. Magnetic Measurements

The magnetization curve of the CI microparticles was obtained using the experimental setup described in Ref. [36]. The results are presented in Figure 5a and show that the relative saturation magnetization was $\sigma_{sCI} \simeq 200$ A·m^2/kg for the values of the magnetic field intensity $H \gtrsim 500$ kA/m.

In the case of the magnetizable CMs with CI, i.e., membranes M_4, M_5, M_6, and M_7, the magnetization curves were obtained by taking into account the fact that between σ_{sCI_i}, with $i = 4, 5, 6, 7$ and the saturation magnetization of the magnetizable CMs σ_{sM_i}, the relation $\sigma_{sM_i} = \Phi_{CI}\mu_0\sigma_{sCI_i}$ [37] holds, where μ_0 is the vacuum magnetic constant; the values of Φ_{CI} are given in Table 1. The resulting magnetization curves are presented in Figure 5b. The data show that σ_{sM_i} were noticeably influenced by the composition of the magnetizable

CMs. Compared with M_4 and M_6, where $\sigma_{sM_4} = \sigma_{sM_6} \simeq 19.78$ A·m^2/kg, for M_5 and M_7 there was an increase of about 100% in the saturation magnetization. This was expected since the volume of the magnetizable phase also increased by the same amount, as seen in Table 1.
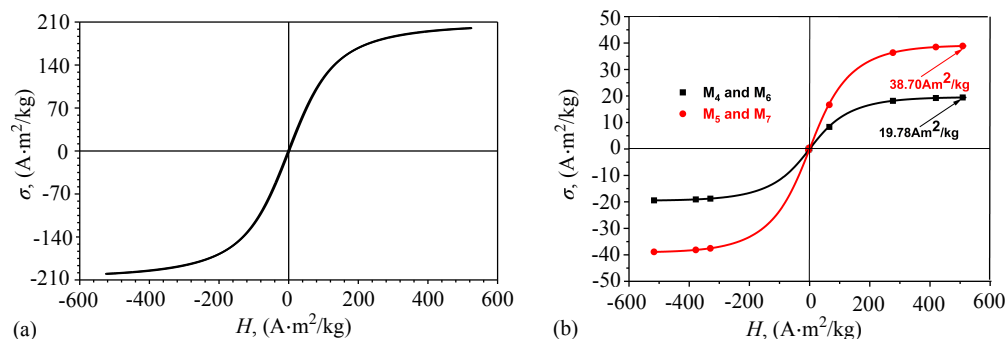

Figure 5. Magnetization curves for the CI microparticles (**a**) and the magnetizable CMs (**b**). σ is the relative magnetization and H is the magnetic field intensity.

6. Fabrication of the Electrical Devices and the Experimental Setup

For the manufacturing of the electrical devices, the following materials were used:

- A textolite plate coated with copper foil on one side, with dimensions of 100 mm × 75 mm × 0.8 mm, from Electronic Light Tech. The thickness of the copper foil was 35 μm and the plate itself was based on epoxy resin, FR40type, reinforced with fiberglass.
- Membranes M_i, with $i = 1, \ldots, 7$ (Table 1) with dimensions of 30 mm × 25 mm × 0.8 mm.

The main steps in their manufacturing process were as follows:

1. Two pieces of dimensions 30 mm × 25 mm × 0.4 mm were cut from the textolite plate, and on each plate, two electrical conductors were welded, as shown in Figure 6.
2. The membranes were placed between each of the two electroconductive plates. As such, the electrical devices ED_i with $i = 4, 5, 6, 7$ were obtained. Figure 7a shows the electrical device with membrane M_3.
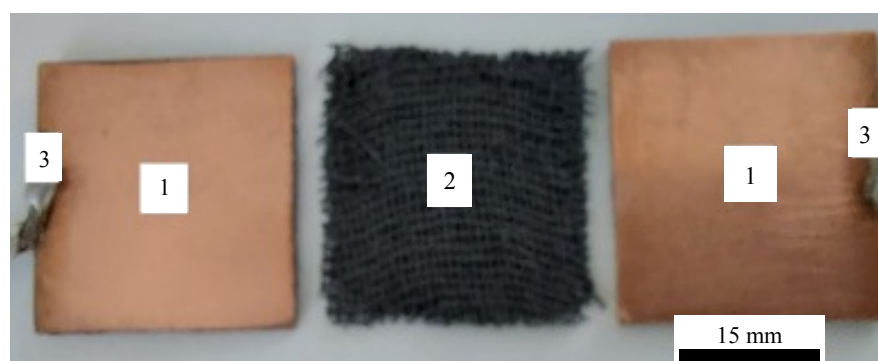

Figure 6. The components of the electrical device: 1—copper coated side of plates, 2—magnetizable CMs, 3—electrical connectors. The image was taken under different illumination conditions than those used for the image in Figure 4.

The experimental setup used for investigating the electrical properties of membranes M_4, M_5, M_6, and M_7 in a medium-frequency electric field superimposed on a static magnetic field is shown in Figure 7b. The setup consisted of an electromagnet with N and S poles. ED_4, ED_5, ED_6, and ED_7 were introduced, in turn, between the N and S poles. Here, the magnetic flux density B was continuously tuned with the help of a direct continuous source (DCS), RXN-3020D type, from Haoxin. The tuning was performed by changing the intensity

of the electrical current passing through the coil of the electromagnet. The maximum value attained by the magnetic flux density was 450 mT. A Hall probe was placed between the electrical device and the S pole of the electromagnet, as shown in Figure 7b, and was connected to a DX-102-type gaussmeter from Dexing Magnets.

The fixation of the electrical device and the Hall probe was carried out by mechanical fixing with a non-magnetic mass (position 5 in Figure 6b). The mechanical tension developed by the non-magnetic body on the surface of the device was about 5 kPa. This value led to good electrical contact between the membranes and copper electrodes of the textolite plates. The electrical properties of the device were measured with the help of an E7−20−type impedancemeter from MNIPI and then they were transferred to a computing unit (not shown in Figure 7b) for further processing. During the measurements, at the terminals of the impedancemeter, the impedance was fixed at 10 MΩ. In order to avoid the electrical breakdown in the membranes, the voltage at the terminals of the electrical devices was fixed at 1 V_{ef}.
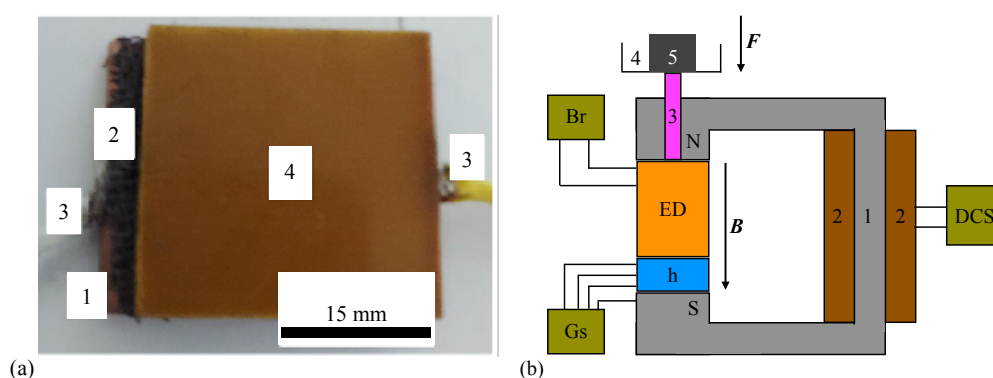

(a)   (b)

Figure 7. (**a**) Assembled electrical device: 1—copper-coated side of plates, 2—magnetizable CMs, 3—electrical connectors, 4—epoxy resin plate reinforced with fiberglass. The image was taken under the same illumination conditions as those used for the image in Figure 5. (**b**) The experimental setup used to measure the electrical properties of the device: 1—magnetic yoke with N and S poles, 2—coil, 3—non-magnetic spindle, 4—non-magnetic plate, 5—non-magnetic weight, DCS—continuous source current, Br—impedancemeter, Gs—gaussmeter, h—Hall probe, **B**—magnetic flux density vector, **F**—gravity force, ED—electrical device.

7. Results

The electrical properties of the devices without CI microparticles (i.e., ED_1, ED_2, and ED_3) were first investigated without the presence of a magnetic flux density. The results for the capacitance and dielectric loss tangent are presented in Figure 8a,b, respectively, and show that both quantities were noticeably influenced by the addition of honey and silver microparticles. For the quantities used (see Table 1), the electrical capacitance when only honey was added (red curve) was about ten times larger compared to the case of the microfibers only (black curve). When silver microparticles were added to honey, the capacitance further increased, on average, by a factor of about 3.5 (blue curve). Similar qualitative behavior also held for the dielectric loss tangent (Figure 8b).

For the investigated membranes, the equivalent electrical resistance R and the electrical resistivity σ were related by

$$R = \frac{h_0}{\sigma L l}, \tag{1}$$

where L, l, and h_0 are the common length, width, and height, respectively, of the electrodes. In addition to Equation (1), the following relations for the electrical conductivity σ, capacitance C, and dielectric loss factor ϵ'' were used [38]:

$$\sigma = 2\pi f \epsilon_0 \epsilon'', \quad C = \epsilon_0 \epsilon' L l / h_0 \quad \text{and} \quad \epsilon'' = \epsilon' D. \tag{2}$$

Then, by using Equation (1), together with the numerical values $L = 30$ mm, $l = 25$ mm, $h_0 = 0.8$ mm, and $\epsilon_0 = 8.845$ pF/m, one obtains

$$R \equiv \frac{1}{2\pi f CD} = \frac{10^6}{2\pi f(\text{kHz})C(\text{pF})D}. \tag{3}$$

The results are shown in Figure 8c and indicate a decrease in the resistance of ED_3 by about three orders of magnitude compared to ED_1.
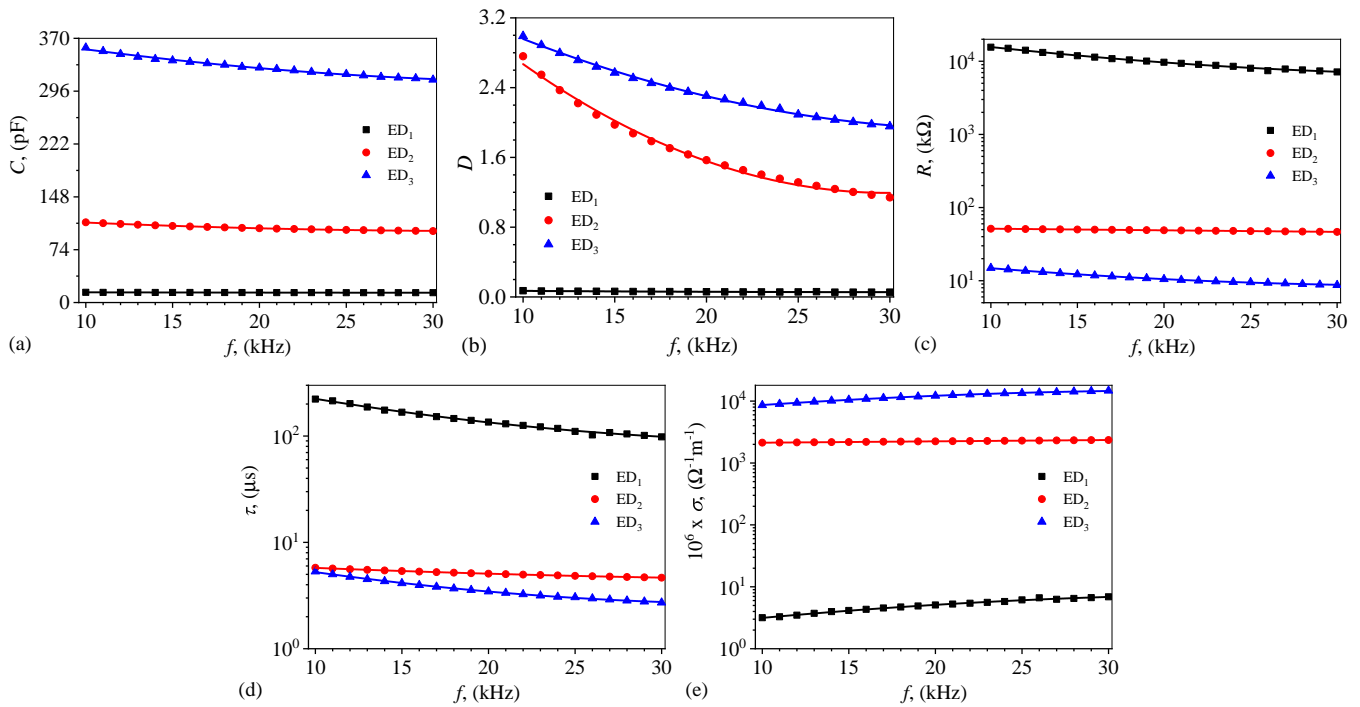

Figure 8. Variations in (**a**) capacitance C, (**b**) dielectric loss tangent D, (**c**) resistance R, (**d**) time constant τ, and (**e**) electrical conductivity σ, of the electrical devices without CI microparticles (i.e., ED_1, ED_2, and ED_3), with the frequency f of a sinusoidal electric field at $B = 0$ mT.

Using Equation (3), the time constant τ of the electrical device, which represents a measure of the storage duration of the electromagnetic energy between the electrodes of the device, is obtained according to

$$10^9 \cdot \tau(\mu s) = C(\text{pF})R(\text{k}\Omega). \tag{4}$$

Then, by introducing the variations $C = C(f)_B$ and $D = D(f)_B$ from Figures 8a,b in the last equation, one obtains the variation in the time constant of the device with the frequency f at fixed values of B, as presented in Figure 8d. The results show that τ decreases with the addition of honey and silver microparticles.

Using the data from Table 2 together with the set of equations given by relation 2, the electrical conductivity becomes

$$\sigma = 2\pi\epsilon_0 D\epsilon' = 2\pi f D \frac{Cd}{S} = 8.373 \cdot d(\text{cm})f(\text{kHz})DC(\text{pF}). \tag{5}$$

The results are shown in Figure 8e and reveal an increase of three orders of magnitude for ED_2, whereas for ED_3, the increase was about four orders of magnitude. In the investigated f-range, in all cases, the conductivity was quasi-constant.

An important factor that affects the properties of these composite membranes is the evaporation of water from honey. Initially, the membrane was found between the two textolite plates, which act as a barrier and prevent evaporation. However, when the

membrane was removed from within the plates for a given period of time, the evaporation process was pronounced enough at room temperature (22 °C), normal ambient humidity (55%), and pressure conditions. In order to investigate these effects, the variations in the capacitance and dielectric loss tangent with the frequency f of the electric field were investigated at various times t after the membrane was manufactured. The results are presented in Figure 9 and show that within several hours, both the capacitance and dielectric loss factor noticeably decreased. In particular, after about six hours, stabilization seemed to be achieved.
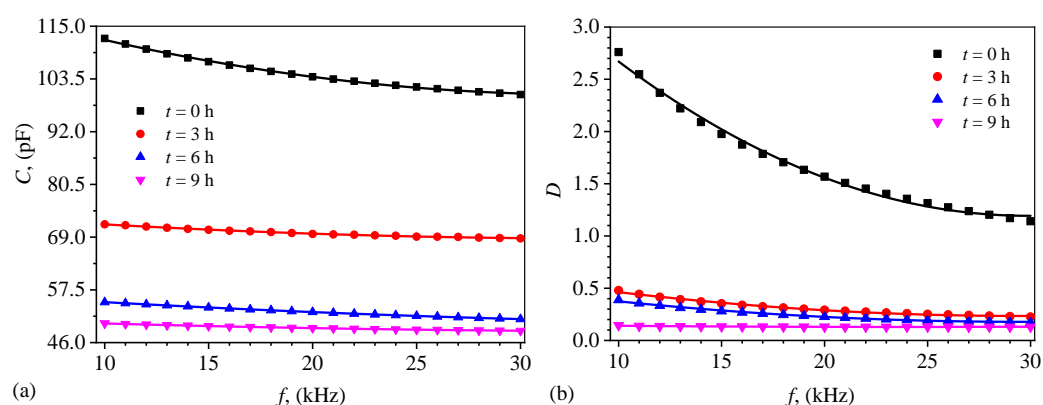

Figure 9. Variations in (**a**) capacitance C, and (**b**) dielectric loss tangent D of the electrical device containing only honey (i.e., ED_2), with the frequency f of a sinusoidal electric field at $B = 0$ mT and at various times t.

The effects of the magnetic field on the electrical properties of the membranes with CI microparticles were determined by measuring the electrical capacitance C and the dielectric loss tangent D of electrical devices ED_4, ED_5, ED_6, and ED_7. The measurements were performed using the impedancemeter, with a fixed input impedance of 10 kΩ and alternating voltage of 1 V_{ef}. The frequency f was adjusted from the control panel of the impedancemeter in steps of 1 kHz. The magnetic field measured with the DX-102 gaussmeter was adjusted from 0 mT to 400 mT in steps of 200 mT. The variation in the capacitance with the frequency of the electric field, i.e., $C = C(f)_B$, is shown in Figure 10, for three values of the magnetic flux density B. Similarly, the variation in the dielectric loss tangent, i.e., $D = D(f)_B$, is shown in Figure 11.

In a magnetic field, CI microparticles become magnetic dipoles almost instantaneously, among which magnetic interactions arise [39]. As a consequence, the dipoles arrange themselves in the form of parallel chains along the height of the membrane. Thus, electrical microcapacitors are made between two magnetic dipoles. They are connected along the dipole chain, having their ends anchored on the copper electrodes. Through these electrodes, the microcapacitors, grouped in series, are electrically connected in parallel. The net effect is an equivalent capacitor whose electrical capacity changes with the increase in the B values of the magnetic flux density, as given in Figure 10.

The addition of silver microparticles to the solution of honey and CI microparticles led to a more conductive solution. For a fixed amount of honey, the conductivity of the mixture increased with the increase in the silver quantity. This was equivalent to the reduction in the distance between the magnetic dipoles and thus, for a fixed value of the magnetic flux density B, the capacitance of the electrical device increased, as shown in Figure 10.
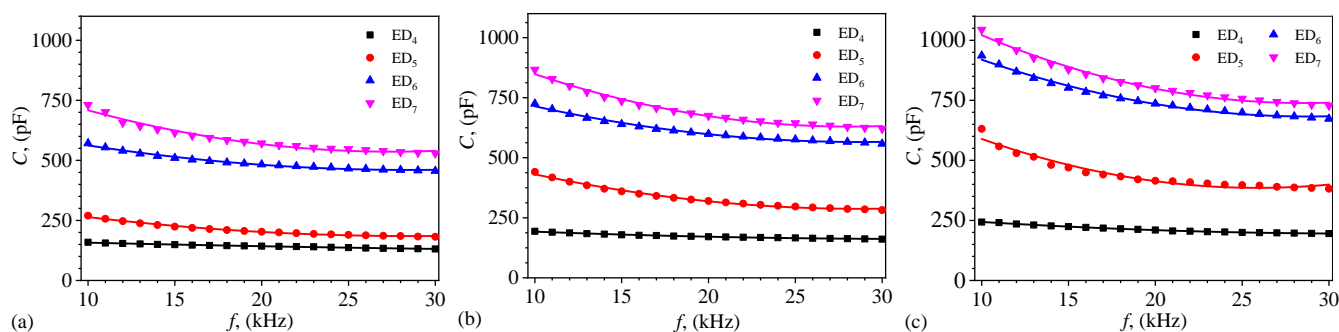
Figure 10. Variations in capacitance C with the frequency f of a sinusoidal electric field at discrete values of the magnetic flux density B. (**a**) $B = 0$ mT. (**b**) $B = 200$ mT. (**c**) $B = 400$ mT.
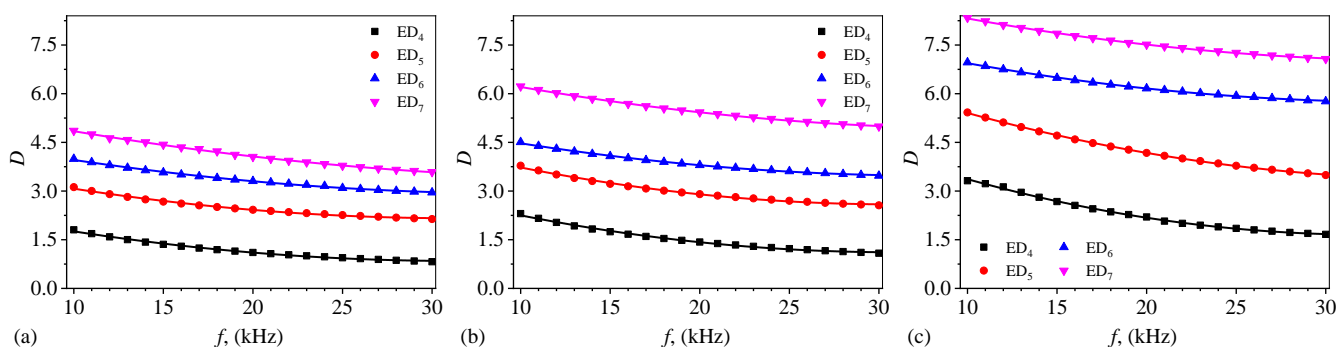

Figure 11. Variations in dielectric loss tangent D with the frequency f of a sinusoidal electric field at discrete values of the magnetic flux density B. (**a**) $B = 0$ mT. (**b**) $B = 200$ mT. (**c**) $B = 400$ mT.

Using the data from Figures 10 and 11 in Equation (3), one obtains the variations in the resistance with frequency f, as shown in Figure 12. The data show that the resistance decreased with the addition of the microparticles. In particular, the highest decrease was at $B = 0$ mT, where the resistance of ED_7 was about one order of magnitude smaller than that of ED_4. When $B \neq 0$, the differences between the resistances of ED_4 and ED_7 were less pronounced. Similar qualitative behavior also held for the time constant (Figure 13). Note that such behavior for the resistance and capacitance can be described qualitatively using models based on dipolar approximation [24].
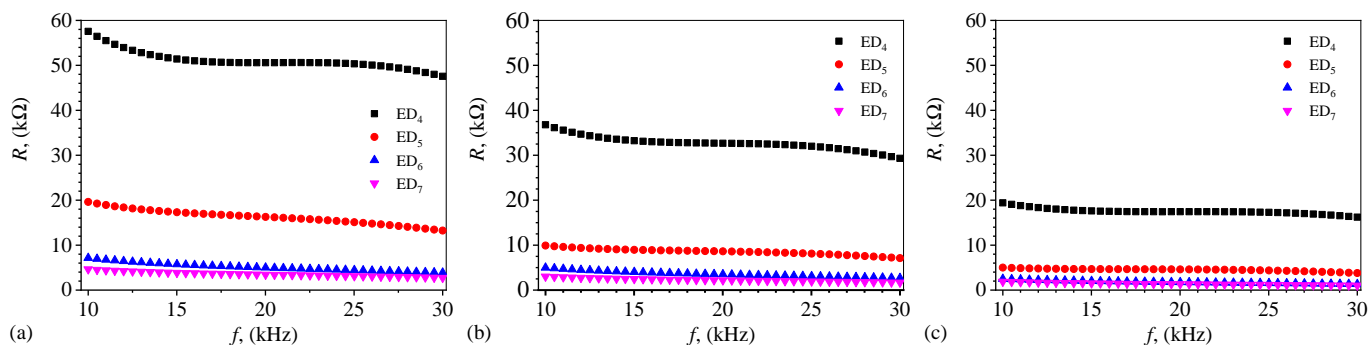

Figure 12. Variations in resistance R with the frequency f of a sinusoidal electric field at discrete values of the magnetic flux density B. (**a**) $B = 0$ mT. (**b**) $B = 200$ mT. (**c**) $B = 400$ mT.
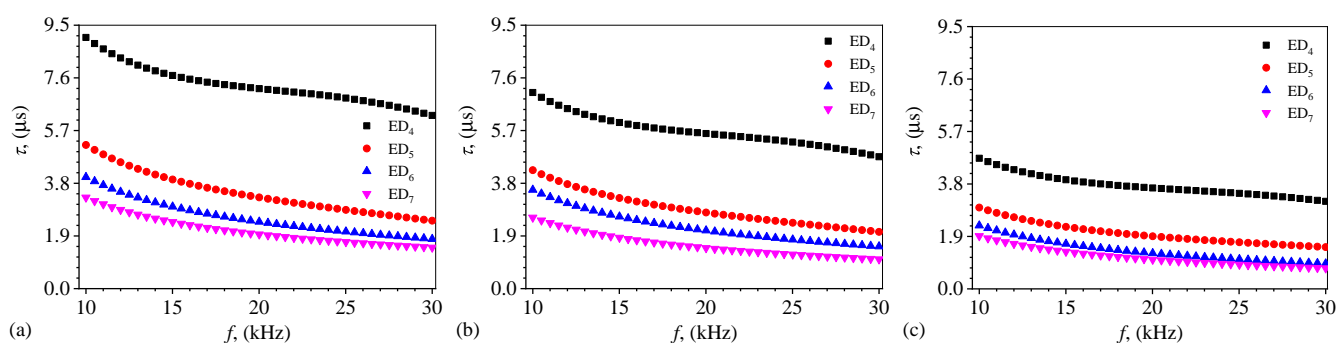
Figure 13. Variations in time constant τ with the frequency f of a sinusoidal electric field at discrete values of the magnetic flux density B. (**a**) $B = 0$ mT. (**b**) $B = 200$ mT. (**c**) $B = 400$ mT.

Finally, the variations in the electrical conductivity with frequency f at fixed values of the magnetic flux density were obtained from the variations in the capacitance (Figure 10) and the dielectric loss factor (Figure 11), used together with Equation (2). The results are presented in Figure 14 and for each electrical device, they indicate a quasi-linear dependence on the frequency f for all values of B. However, the addition of CI and silver microparticles led to a faster increase in the conductivity, starting from higher initial values. In particular, the fastest increase was for ED_7 at $B = 400$ mT, with an initial starting point of about $0.9\ \Omega^{-1}\text{m}^{-1}$ at $f = 10$ kHz. Moreover, at a fixed value of f, the electrical conductivity increased with both B and the quantity of silver microparticles. Thus, through electrical conductivity, one can control the drug-release process of biocomponents from honey with the help of f, B, and the quantity of silver microparticles.
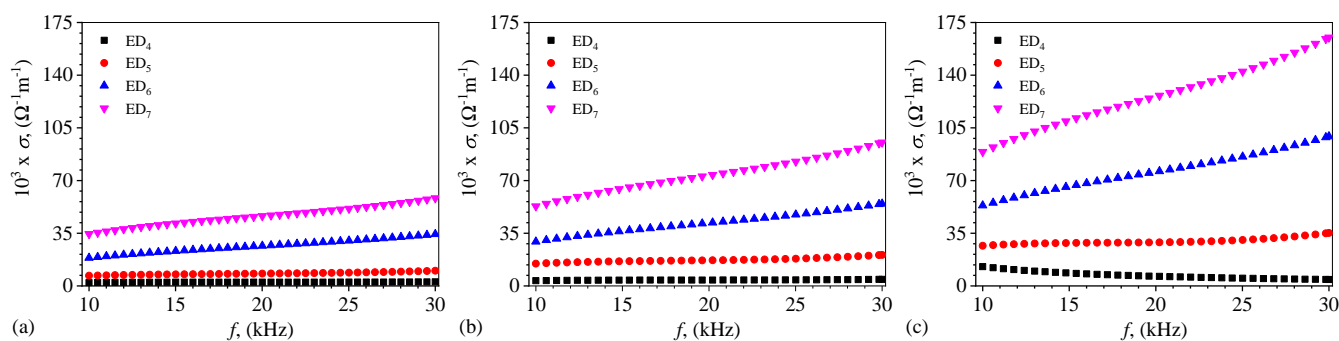

Figure 14. Variations in electrical conductivity σ with the frequency f of a sinusoidal electric field at discrete values of the magnetic flux density B. (**a**) $B = 0$ mT. (**b**) $B = 200$ mT. (**c**) $B = 400$ mT.

8. Discussion

The increase in the capacitance (Figure 10) and the decrease in the resistance (Figure 12) with the magnetic flux density arise because CI microparticles become magnetic dipoles when the magnetic field is applied. They are oriented along the magnetic field lines and form aggregates in the form of parallel and equidistant chain-like structures, as reported in Refs. [27,40]. As such, each pair of magnetic dipoles forms an electric microcapacitor and at the same time, an electric microresistor. Within each chain, they are connected in series, whereas through the copper foils on the textolite plates, they are connected in parallel. When the magnetic field is applied, interactions are established between the magnetic dipoles, and as a result, the distance between them decreases with an increasing magnetic flux density [27,40]. Thus, the net effect of the magnetic field is the increase in the electrical capacitance and decrease in the electrical resistance of the microelements of the electrical circuit within the body of the electrical devices. Further, by decreasing the distance between metallic microparticles, the honey film reduces its thickness. Then, the contact electrical resistance between the microparticles in the chains decreases, which is equivalent to a decrease in the height of the electrical potential well [41]. In this way, electrons from lower

energy levels pass over the potential well, leading to the observed increase/decrease in the electrical capacitance/resistance.

Combining these electrical properties with the biomechanical ones in a single membrane gives them a competitive advantage over similar materials. In particular, the use of natural components is not harmful to biological life and does not produce pollution, whereas the structure and composition of cotton microfibers impart a high degree of flexibility to the whole membrane.

Refs. [42,43], for example, reported the fabrication of electrical devices based on cotton microfibers soaked in magnetorheological suspensions consisting of liquid solutions with CI microparticles and various additives such as silicone oil. The reported results showed that the electrical capacitance and resistance were noticeably modified by the magnetic flux density and the volume fraction of the CI. However, the essential difference is that the components used in the above-mentioned works were environmentally unfriendly.

To alleviate this issue, Refs. [44,45] reported the fabrication of membranes based on non-polluting components, which are useful for various technical and medical applications. Similar to the results reported here, the electrical and viscoelastic properties were shown to be noticeably influenced by the magnetic flux density and volume fractions of the used components. In Ref. [44], membranes based on honey, CI microparticles, and turmeric powder as additives were produced. The reported electrical properties depended on the volume concentration of the turmeric powder and the existence of the maxima of the dielectric losses was revealed. This provided the possibility of heating the membrane in a medium-frequency electric field superimposed on a static magnetic field so that the natural components could be selectively released depending on the application. Ref. [45] reported the results of membranes based on medical gauze bandages soaked in honey and CI microparticles. It was shown that by the application of a magnetic field, the transmission of white light could be tuned and by superimposing a medium-frequency electric field over a static magnetic field, the membranes could be heated so that the natural components from honey could also be selectively released. Compared to the membranes reported in Refs. [44,45], the membranes manufactured in this work have electrical properties that can be sensitively tuned. Moreover, the antiseptic properties of silver microparticles are useful for the fabrication of various medical devices.

9. Conclusions

In this work, a new type of low-cost, biodegradable, and environmentally friendly membrane based on cotton microfibers, honey, CI microparticles, and various quantities of silver microparticles are manufactured. The membranes are used as dielectric materials for the fabrication of electrical devices in the form of plane electrical capacitors, and the effects of an external magnetic field on the electrical capacitance C, dielectric loss tangent D, resistance R, time constant τ, and electrical conductivity σ are investigated.

The magnetic flux density is varied in steps of 200 mT from 0 to 400 mT. The measurements are performed in a medium-frequency alternating electric field with frequencies varying in steps of 1 kHz from 10 kHz to 30 kHz using a new in-house experimental setup, designed and built for these types of measurements.

It is shown that all the measured quantities are noticeably influenced by the frequency of the electric field, the magnetic flux density, and the volume concentration of the silver and CI microparticles. By increasing the frequency of the electric field, the values of all electrical properties are decreased. The most pronounced decrease is in the small values of the frequencies, in general, smaller than 10–12 kHz. However, an increase in the magnetic flux density and mass concentration of silver microparticles increases the values of the electrical properties, except for the time constant, which decreases with an increase in the magnetic flux density.

These results show that the electrical properties of the obtained membranes can be tuned remotely. In particular, the dielectric loss factor and electrical conductivity show that

the membranes can be heated up for an electrically and/or magnetically controlled release of bioactive compounds from honey.

Taking into account their chemical compositions and the very small values of the magnetic field density, which the membrane can sense, they are very good candidates for the fabrication of devices that are useful for biomedical applications or electromagnetic shielding. In particular, the method of preparing magnetizable membranes can be useful for the realization of technologies that can follow the crystallization kinetics of bee honey and the detection of impurities. The decrease in the electrical resistance suggests the possibility of manufacturing medical devices in which bee honey, CI, and silver particles are used in dermatological treatments. Thus, by choosing the composition of the membranes and/or the value of the magnetic flux density, the value of the intensity of the electric current through the electrical device can be fixed. In this way, it is possible to obtain a thermal field to facilitate the penetration of useful substances from the membranes into the treatment area as required.

Author Contributions: Conceptualization, I.B.; methodology, I.B. and E.M.A.; validation, I.B. and E.M.A.; formal analysis, I.B. and E.M.A.; data curation, E.M.A.; writing—original draft preparation, I.B.; writing—review and editing, E.M.A.; visualization, E.M.A.; investigation SEM and EDX analysis, P.S. All authors have read and agreed to the published version of the manuscript.

Abbreviations

The following abbreviations are used in this manuscript:

| CMs | Composite membranes |
| CI | Carbonyl iron |

References

1. Zahid, M.; Rashid, A.; Akram, S.; Rehan, Z.A.; Razzaq, W. A Comprehensive Review on Polymeric Nano-Composite Membranes for Water Treatment. *J. Membr. Sci. Technol.* **2018**, *8*, 1000179. [CrossRef]
2. Wang, X.; Wang, N.; Li, X.; An, Q.F. A review of nano-confined composite membranes fabricated inside the porous support. *Adv. Membr.* **2021**, *1*, 100005. [CrossRef]
3. Liu, L.; Tong, C.; He, Y.; Zhao, Y.; Lü, C. Enhanced properties of quaternized graphenes reinforced polysulfone based composite anion exchange membranes for alkaline fuel cell. *J. Membr. Sci.* **2015**, *487*, 99–108. [CrossRef]
4. Huiya, W.; Ran, G.; Xinliang, Q. Preparation and Characterization of TiO_2/g-C3N4/PVDF Composite Membrane with Enhanced Physical Properties. *Membranes* **2018**, *8*, 14.
5. Qadir, A.; Le, T.K.; Malik, M.; Min-Dianey, K.A.A.; Saeed, I.; Yu, Y.; Choi, J.R.; Pham, P.V. Representative 2D-material-based nanocomposites and their emerging applications: A review. *RSC Adv.* **2021**, *11*, 23860–23880. [CrossRef]
6. Ng, C.Y.; Ng, L.Y.; Mahmoudi, E.; Chung, Y.T. Fabrication of graphene-based membrane for separation of hazardous contaminants from wastewater. In *Graphene-Based Nanotechnologies for Energy and Environmental Applications*; Jawaid, M., Ahmad, A., Lokhat, D., Eds.; Elsevier: Amsterdam, The Netherlands, 2019; pp. 267–291. [CrossRef]
7. Iojoiu, C.; Danyliv, O.; Alloin, F. Ionic Liquids and Polymers for Battery and Fuel Cells. In *Modern Synthesis Processes and Reactivity of Fluorinated Compounds*; Groult, H., Leroux, F.R., Tressaud, A., Eds.; Elsevier: Amsterdam, The Netherlands, 2019; pp. 465–497. [CrossRef]
8. Fatima, A.; Yasir, S.; Khan, M.S.; Manan, S.; Ullah, W.; Ul-Islam, M. Plant extract-loaded bacterial cellulose composite membrane for potential biomedical applications. *J. Bioresour. Bioprod.* **2021**, *6*, 26–32. [CrossRef]
9. Kim, S.; Wang, H.; Lee, Y.M. 2D Nanosheets and Their Composite Membranes for Water, Gas, and Ion Separation. *Angew. Chem.* **2019**, *131*, 17674–17689. [CrossRef]

10. Elmahaisi, M.F.; Azis, R.S.; Ismail, I.; Muhammad, F.D. A review on electromagnetic microwave absorption properties: Their materials and performance. *J. Mater. Res. Technol.* **2022**, *20*, 2188–2220. [CrossRef]

11. Wu, S.; Hu, W.; Ze, Q.; Sitti, M; Zhao, R. Multifunctional magnetic soft composites: A review. *Multifunct. Mater.* **2020**, *3*, 042003. [CrossRef]

12. Abdalla, I.; Yu, J.; Li, Z.; Ding, B. Nanofibrous membrane constructed magnetic materials for high-efficiency electromagnetic wave absorption. *Compos. Part B Eng.* **2018**, *155*, 397–404. [CrossRef]

13. Haye, E.; Soon Chang, C.; Dudek, G.; Hauet, T.; Ghanbaja, J.; Busby, Y.; Job, N.; Houssiau, L.; Pireaux, J.-J. Tuning the Magnetism of Plasma-Synthesized Iron Nitride Nanoparticles: Application in Pervaporative Membranes. *ACS Appl. Nano Mater.* **2019**, *2*, 2484–2493. [CrossRef]

14. Salidkul, N.; Mongkolthanaruk, W.; Faungnawakij, K.; Pinitsoontorn, S. Hard magnetic membrane based on bacterial cellulose— Barium ferrite nanocomposites. *Carbohydr. Polym.* **2021**, *264*, 118016. [CrossRef] [PubMed]

15. Dongre, R.S.; Sadasivuni, K.K.; Deshmukh, K.; Mehta, A.; Basu, S.; Mashram, J.S.; Al-Maadeed, M.A.A.; Karim, A. Natural polymer based composite membranes for water purification: A review. *Polym.-Plast. Tech. Mat.* **2019**, *58*, 1295–1310. [CrossRef]

16. Xue, Y.; Lofland, S.; Xiao, H. Comparative Study of Silk-Based Magnetic Materials: Effect of Magnetic Particle Types on the Protein Structure and Biomaterial Properties. *Int. J. Mol. Sci.* **2020**, *21*, 7583. [CrossRef]

17. Giannelli, M.; Barbalinardo, M.; Riminucci, A.; Belvedere, K.; Boccalon, E.; Sotgiu, G.; Corticelli, F.; Ruani, G.; Zamboni, R.; Aluigi, A.; et al. Magnetic keratin/hydrotalcites sponges as potential scaffolds for tissue regeneration. *Appl. Clay Sci.* **2021**, *207*, 106090. [CrossRef]

18. Sriplai, N; Prinitsoontorn, S. Bacterial cellulose-based magnetic nanocomposites: A review. *Carbohydr. Polym.* **2021**, *254*, 117228. [CrossRef]

19. Patiño-Ruiz, D.; Sanchez-Botero, L.; Hinestroza, J.; Herrera, A. Modification of Cotton Fibers with Magnetite and Magnetic Core-Shell Mesoporous Silica Nanoparticles. *Phys. Status Solidi A* **2018**, *215*, 1800266. [CrossRef]

20. DeFrates, K.G.; Moore, R.; Borgesi, J.; Lin, G.; Mulderig, T.; Beachley, V.; Hu, X. Protein-Based Fiber Materials in Medicine: A Review. *Nanomaterials* **2018**, *8*, 457. [CrossRef]

21. Bealer, E.J.; Kavetsky, K.; Dutko, S.; Lofland, S.; Hu, X. Protein and Polysaccharide-Based Magnetic Composite Materials for Medical Applications. *Int. J. Mol. Sci.* **2020**, *21*, 186. [CrossRef]

22. Varghese, A.M.; Mittal, V. Surface modification of natural fibers. In *Biodegradable and Biocompatible Polymer Composites*; Shimpi, N.G., Ed.; Woodhead Publishing: Sawston, UK, 2018; pp. 115–155. [CrossRef]

23. Dochia, M.; Sirghie, C.; Kozłowski, R.M.; Roswitalski, Z. Cotton fibres. In *Handbook of Natural Fibres*; Kozłowski, R.M., Ed.; Woodhead Publishing: Sawston, UK, 2012; pp. 11–23. [CrossRef]

24. Bica, I; Anitas, E. M; Chirigiu, L. Hybrid Magnetorheological Composites for Electric and Magnetic Field Sensors and Transducers. *Nanomaterials* **2020**, *10*, 2060. [CrossRef]

25. Bunoiu, O.M.; Anitas, E.M.; Pascu, G.; Chirigiu, L.M.E.; Bica, I. Electrical and Magnetodielectric Properties of Magneto-Active Fabrics for Electromagnetic Shielding and Health Monitoring. *Int. J. Mol. Sci.* **2020**, *13*, 4785. [CrossRef] [PubMed]

26. Iacobescu, G.E.; Bica, I.; Chirigiu, L.M.E. Physical Mechanisms of Magnetic Field Effects on the Dielectric Function of Hybrid Magnetorheological Suspensions. *Materials* **2021**, *14*, 6498. [CrossRef] [PubMed]

27. Pascu, G.; Bunoiu, O.M.; Bica, I. Cotton fibres. Magnetic Field Effects Induced in Electrical Devices Based on Cotton Fiber Composites, Carbonyl Iron Microparticles and Barium Titanate Nanoparticles. *Nanomaterials* **2022**, *12*, 888. [CrossRef]

28. Bica, I; Anitas, E.M. Electrical devices based on hybrid membranes with mechanically and magnetically controllable, resistive, capacitive and piezoelectric properties. *Smart Mater. Struct.* **2022**, *31*, 045001. [CrossRef]

29. Cai, Q.; Yang, S.; Zhang, C.; Li, Z.; Li, X.; Shen, Z.; Zhu, W. Facile and Versatile Modification of Cotton Fibers for Persistent Antibacterial Activity and Enhanced Hygroscopicity. *ACS Appl. Mater.* **2018**, *10*, 38506–38516. [CrossRef]

30. Cianciosi, D.; Forbes-Hernández, T.Y.; Afrin, S.; Gasparrini, M.; Reboredo-Rodriguez, P.; Manna, P.P.; Zhang, J.; Bravo, L.L.; Martinéz F. S.; Agudo, T.P.; et al. Phenolic Compounds in Honey and Their Associated Health Benefits: A Review. *Molecules* **2018**, *23*, 2322. [CrossRef]

31. Plachy, T.; Cvek, M.; Munstr, L., Hanulikova, B.; Suly, P.; Vesel, A.; Cheng, Q. Enhanced magnetorheological effect of suspensions based on carbonyl iron particles coated with poly (amidoamine) dendrons. *Rheol. Acta* **2021**, *60*, 263–276. [CrossRef]

32. Salem, A.M.H.; Ali, A.; Ramli, R.B.; Muthalif, A.G.A.; Julai, S. Effect of Carbonyl Iron Particle Types on the Structure and Performance of Magnetorheological Elastomers: A Frequency and Strain Dependent Study. *Polymers* **2022**, *14*, 4193. [CrossRef]

33. Sista, K.S.; Dwarapudi, S.; Kumar, D.; Sinha, G.R.; Moon, A.P. Carbonyl iron powders as absorption material for microwave interference shielding: A review. *J. Alloys Compd.* **2021**, *853*, 157251. [CrossRef]

34. Briguglio, M.; Hrelia, S.; Malaguti, M.; De Vecchi, E.; Lombardi, G.; Banfi, G.; Riso, P.; Porrini, M.; Romagnoli, S.; Pino, F.; et al. Oral Supplementation with Sucrosomial Ferric Pyrophosphate Plus L-Ascorbic Acid to Ameliorate the Martial Status: A Randomized Controlled Trial. *Nutrients* **2020**, *12*, 386. [CrossRef]

35. Bruna, T.; Maldonado-Bravo, F.; Jara, P.; Caro, N. Silver Nanoparticles and Their Antibacterial Applications. *Int. J. Mol. Sci.* **2021**, *22*, 7202. [CrossRef] [PubMed]

36. Ercuta, A. Sensitive AC Hysteresigraph of Extended Driving Field Capability. *IEEE Trans. Instrum. Meas.* **2020**, *69*, 1643–1651. [CrossRef]

37. Genç, S. Synthesis and Properties of Magnethoreological (MR) Fluids. Ph.D. Thesis; University of Pitsburgh, Pittsburgh, PA, USA, 2003; p. 23.
38. Chen, L.F.; Ong, C.K.; Neo, C.P.; Varadan, V.V.; Varadan, V.K. *Microwave Electronics: Measurement and Materials Characterization*, 1st ed.; Wiley: Hoboken, NJ, USA, 2004.
39. Bica, I.; Anitas, E.M.; Averis, L.M.E. Tensions and deformations in composites based on polyurethane elastomer and magnetorheological suspension: Effects of the magnetic field. *J. Ind. Eng. Chem.* **2015**, *28*, 86–90. [CrossRef]
40. Bica, I.; Anitas, E.M. Magnetic field and microstructural effects on the electrical capacitance and resistance of a quadrupolar electrical capacitor based on cotton fabrics and carbonyl iron microparticles. *Smart Mater. Struct.* **2022**, *31*, 125018. [CrossRef]
41. Kchit, N.; Bossis, G. Electrical resistivity mechanism in magnetorheological elastomer. *J. Phys. D Appl. Phys.* **2009**, *42*, 105505. [CrossRef]
42. Bica, I.; Anitas, E.M. Magnetic field intensity and γ-Fe_2O_3 concentration effects on the dielectric properties of magnetodielectric tissues *Mater. Sci. Eng. B* **2018**, *236–237*, 125–131. [CrossRef]
43. Bica, I.; Anitas, E.M.; Chirigiu, L.; Daniela, C; Chirigiu, L.M.E. Hybrid magnetorheological suspension: Effects of magnetic field on the relative dielectric permittivity and viscosity *Colloid Polym. Sci.* **2018**, *296*, 1373–1378. [CrossRef]
44. Bica, I.; Anitas, E.M. Magnetic field intensity effect on electrical conductivity of magnetorheological biosuspensions based on honey, turmeric and carbonyl iron *J. Ind. Eng. Chem.* **2018**, *64*, 276–283. [CrossRef]
45. Bica, I.; Anitas, E.M. Light transmission, magnetodielectric and magnetoresistive effects in membranes based on hybrid magnetorheological suspensions in a static magnetic field superimposed on a low/medium frequency electric field *J. Magn. Magn. Mater.* **2020**, *511*, 166975. [CrossRef]